

# Glucagon Regulation of Oxidative Phosphorylation Requires an Increase in Matrix Adenine Nucleotide Content through $\text{Ca}^{2+}$ Activation of the Mitochondrial ATP-Mg/ $\text{P}_i$ Carrier S $\text{CaMC-3}^*$

Received for publication, August 8, 2012, and in revised form, January 14, 2013. Published, JBC Papers in Press, January 23, 2013, DOI 10.1074/jbc.M112.409144

Ignacio Amigo<sup>†§1</sup>, Javier Traba<sup>†§2</sup>, M. Mar González-Barroso<sup>¶</sup>, Carlos B. Rueda<sup>†§</sup>, Margarita Fernández<sup>||</sup>, Eduardo Rial<sup>¶</sup>, Aránzazu Sánchez<sup>||</sup>, Jorgina Satrustegui<sup>†§3</sup>, and Araceli del Arco<sup>\*\*4</sup>

From the <sup>†</sup>Departamento de Biología Molecular, Centro de Biología Molecular Severo Ochoa, Universidad Autónoma de Madrid-CSIC, <sup>§</sup>Centro de Investigaciones Biomédicas en Red de Enfermedades Raras (CIBERER) 28049 Madrid, and <sup>¶</sup>Departamento de Medicina Celular y Molecular, Centro de Investigaciones Biológicas (CIB), Consejo Superior de Investigaciones Científicas 28040 Madrid, the <sup>||</sup>Departamento de Bioquímica y Biología Molecular II, Facultad de Farmacia, Universidad Complutense de Madrid 28040 Madrid, and the <sup>\*\*</sup>Área de Bioquímica, Centro Regional de Investigaciones Biomédicas, Facultad de Ciencias Ambientales y Bioquímica, Universidad de Castilla La Mancha (UCLM), Avda. Carlos III s/n, Toledo 45071, Spain

**Background:** Glucagon stimulates liver respiration.

**Results:** S $\text{CaMC-3}$  is the only functional mitochondrial ATP-Mg/ $\text{P}_i$  carrier in adult liver and S $\text{CaMC-3}$  deficiency prevents glucagon effects in hepatocytes and *in vivo*.

**Conclusion:** S $\text{CaMC-3}$  is required for the stimulation of oxidative phosphorylation in response to glucagon through a  $\text{Ca}^{2+}$ -dependent increase of mitochondrial adenine nucleotides and  $\text{Ca}^{2+}$  retention.

**Significance:**  $\text{Ca}^{2+}$  stimulation of S $\text{CaMC-3}$  is required for liver response to glucagon.

It has been known for a long time that mitochondria isolated from hepatocytes treated with glucagon or  $\text{Ca}^{2+}$ -mobilizing agents such as phenylephrine show an increase in their adenine nucleotide (AdN) content, respiratory activity, and calcium retention capacity (CRC). Here, we have studied the role of S $\text{CaMC-3}/\text{slc}25\text{a}23$ , the mitochondrial ATP-Mg/ $\text{P}_i$  carrier present in adult mouse liver, in the control of mitochondrial AdN levels and respiration in response to  $\text{Ca}^{2+}$  signals as a candidate target of glucagon actions. With the use of S $\text{CaMC-3}$  knock-out (KO) mice, we have found that the carrier is responsible for the accumulation of AdNs in liver mitochondria in a strictly  $\text{Ca}^{2+}$ -dependent way with an  $\text{S}_{0.5}$  for  $\text{Ca}^{2+}$  activation of  $3.3 \pm 0.9 \mu\text{M}$ . Accumulation of matrix AdNs allows a S $\text{CaMC-3}$ -dependent increase in CRC. In addition, S $\text{CaMC-3}$ -dependent accumulation of AdNs is required to acquire a fully active state 3 respiration in AdN-depleted

liver mitochondria, although further accumulation of AdNs is not followed by increases in respiration. Moreover, glucagon addition to isolated hepatocytes increases oligomycin-sensitive oxygen consumption and maximal respiratory rates in cells derived from wild type, but not S $\text{CaMC-3-KO}$  mice and glucagon administration *in vivo* results in an increase in AdN content, state 3 respiration and CRC in liver mitochondria in wild type but not in S $\text{CaMC-3-KO}$  mice. These results show that S $\text{CaMC-3}$  is required for the increase in oxidative phosphorylation observed in liver mitochondria in response to glucagon and  $\text{Ca}^{2+}$ -mobilizing agents, possibly by allowing a  $\text{Ca}^{2+}$ -dependent accumulation of mitochondrial AdNs and matrix  $\text{Ca}^{2+}$ , events permissive for other glucagon actions.

During fasting, glucagon secreted by  $\alpha$ -cells in the pancreas activates a complex metabolic response in liver cells that includes glycogen breakdown, gluconeogenesis, urea synthesis, uptake of adenine nucleotides (AdNs),<sup>5</sup> and increase in the  $\text{Ca}^{2+}$  retention capacity (CRC) of the mitochondria, and stimulation of oxidative phosphorylation (OXPHOS) (1, 2). Although the primary pathway of glucagon action involves binding of the hormone to a G-protein-coupled receptor and formation of cAMP through activation of adenylate cyclase, a cytosolic  $\text{Ca}^{2+}$  signal is also produced both by release of intra-

\* This work was supported in part by Ministerio de Educación y Ciencia Grants BFU2008-04084/BMC and BFU2011-30456, European Union Grant LSHM-CT-2006-518153, and CIBERER Centro de Investigaciones Biomédicas en Red de Enfermedades Raras (an initiative of the ISCIII Instituto de Salud Carlos III) (to J. S.), Comunidad de Madrid Grants S-GEN-0269-2006 and S2010/BMD-2402 MITOLAB-CM (to J. S., E. R., and A. S.), by ISCIII Grant PI080610 (to A. delA), and an institutional grant from the Fundación Ramon Areces to the Centro de Biología Molecular Severo Ochoa.

<sup>1</sup> Recipient of a Formación de Personal Investigador fellowship from the Ministerio de Educación y Ciencia.

<sup>2</sup> Present address: Center for Molecular Medicine, NHLBI, National Institutes of Health, Bethesda, MD.

<sup>3</sup> To whom correspondence may be addressed: Centro de Biología Molecular Severo Ochoa, c/o Nicolás Cabrera 1, Madrid 28049, Spain. Tel.: 34-911-96-4621; Fax: 34-911-96-4420; E-mail: jsatrustegui@cbm.uam.es.

<sup>4</sup> To whom correspondence may be addressed: Facultad de Ciencias Ambientales y Bioquímica, Universidad de Castilla La Mancha, Avda. Carlos III s/n, Toledo 45071, Spain. Tel.: 34-925-26-8800; Fax: 34-925-26-8840; E-mail: araceli.arco@uclm.es.

<sup>5</sup> The abbreviations used are: AdN, adenine nucleotides; KO, knock-out; OXPHOS, oxidative phosphorylation; ANT, ATP/ADP translocase; RR, ruthenium red; S $\text{CaMC}$ , short calcium-binding mitochondrial carrier; FCCP, carbonyl cyanide-4-(trifluoromethoxy)phenylhydrazone; CRC, calcium retention capacity; OCR, oxygen consumption rate; TMPD, *N,N,N',N'*-tetramethyl-*p*-phenylenediamine.

## SCaMC-3 Is a Mitochondrial Target of Glucagon

cellular stores and  $\text{Ca}^{2+}$  entry in the cell (3). Inhibition of this  $\text{Ca}^{2+}$  signal has been shown to block the increase in mitochondrial AdN content after glucagon treatment (4), thereby reducing matrix availability for AdN-dependent reactions, including OXPHOS (5). Two different mechanisms have been proposed to mediate the mitochondrial uptake of AdNs by  $\text{Ca}^{2+}$ . In the first, entry of cytosolic  $\text{Ca}^{2+}$  into the mitochondria would inhibit the matrix pyrophosphatase, leading to an increase in pyrophosphate that would then be exchanged by cytosolic AdNs through the ATP/ADP translocase (ANT) (6). The second mechanism, proposed by Aprille and co-workers (7, 8), involves the ATP-Mg/ $\text{P}_i$  carrier, a  $\text{Ca}^{2+}$ -dependent mitochondrial carrier that has been recently identified at the molecular level (9, 10).

Due to its structure, with  $\text{Ca}^{2+}$ -binding EF-hand domains facing the intermembrane space, the ATP-Mg/ $\text{P}_i$  carrier is activated by  $\text{Ca}^{2+}$  signals that do not require entry of the cation in the mitochondria (reviewed in Ref. 11). To date, five different paralogs, termed SCaMC (short calcium-binding mitochondrial carrier) 1-3, -1-like and -3-like, have been described in mammals (9, 10, 12-14), of which two, SCaMC-1-like and SCaMC-3-like, are only expressed in testis. In addition, several splicing isoforms have been described (9), making it the most complex subgroup of mitochondrial carriers (15). The transport activity catalyzed by the SCaMCs is the electroneutral and reversible exchange of ATP-Mg $^{2-}$  or HADP $^{2-}$  with  $\text{HPO}_4^{2-}$  (16). Unlike the ANT, the ATP-Mg/ $\text{P}_i$  carrier does not interchange AdNs between the cytoplasm and the mitochondria, but rather increases or decreases the net mitochondrial AdN content.

In this work we have studied the role of SCaMC-3/*Slc25a23*, the main paralog of the ATP-Mg/ $\text{P}_i$  carrier in liver, in mitochondrial function in response to  $\text{Ca}^{2+}$ -mobilizing agonists glucagon and phenylephrine. With the use of SCaMC-3 knockout (KO) mice, we have found that the carrier is responsible for the accumulation of AdNs in liver mitochondria in a strictly  $\text{Ca}^{2+}$ -dependent way, with an  $S_{0.5}$  for  $\text{Ca}^{2+}$  activation of  $3.3 \pm 0.9 \mu\text{M}$ , and that SCaMC-3-dependent accumulation of AdNs is required to increase mitochondrial CRC and acquire a fully active state 3 respiration in liver mitochondria. Moreover, glucagon addition to isolated hepatocytes increases oligomycin-sensitive oxygen consumption in cells derived from wild type, but not SCaMC-3-KO mice, and *in vivo* glucagon administration results in an increase in AdN content, CRC, and respiratory capacity in liver mitochondria, mediated by SCaMC-3. These results reveal an important role of SCaMC-3 as a target of  $\text{Ca}^{2+}$ -mobilizing agents in liver by modulating OXPHOS.

### EXPERIMENTAL PROCEDURES

**Animals**—Mice deficient in SCaMC-3 were generated by Lexicon with a mixed C57BL6/Sv129 genetic background. Animals are born in mendelian proportions and show no evident phenotypic traits. Genotyping was performed by double PCR using primers 9 (forward, 5'-TGAGGCATGAGGCATATTCTA-3') and 10 (reverse, 5'-AAGGCTGTGAAACATGAGCA-3') to detect the wild type allele, and primers Neo3a (forward, 5'-GCAGCGCATCGCCTTCTATC-3') and 12 (reverse, 5'-GGGCTAGCTGTATTACCAGTC-3') to detect the targeted

locus. Products were resolved by electrophoresis in 1.5% agarose gels and identified by their fragment sizes. All animal work performed in this study was carried out in accordance with procedures approved in the Directive 86/609/EEC of the European Union and with approval of the Ethics Committee of the Universidad Autónoma de Madrid. Glucagon (2 mg/kg; Sigma) was injected intraperitoneally in fed 3-5-month-old male mice and animals were sacrificed by cervical dislocation 15 min after administration.

**Metabolic Measurements**—Glucose was measured using a blood dropper with Accutrend stripes. Blood serum was obtained from 2-3-month-old wild type and SCaMC-3-KO mice and urea was measured using a commercial kit (Spinreact, Barcelona).

**Hepatocytes Isolation and Culture**—Hepatocytes were isolated as previously described (17). Briefly, livers from 12-h fasted 3-5-month-old male mice were perfused with Hanks' balanced salt solution supplemented with 10 mM Hepes and 0.2 mM EGTA for 5 min, followed by a longer perfusion (10-15 min) with William's medium E containing 10 mM Hepes and 0.03% collagenase H (0.19 units/mg; Sigma). Livers were further minced and viable hepatocytes were selected by centrifugation in Percoll, and seeded in collagen I-coated plates at a density of  $0.6 \times 10^6$  cells/cm $^2$  in Dulbecco's modified Eagle's medium/F-12 (1:1). Cells were kept overnight at 37 °C and 5% CO $_2$ , and used 12-16 h later.

**Western Blot and Antibodies**—Protein samples were collected in extraction buffer (250 mM sucrose, 1 mM EDTA, 1 mM EGTA, 25 mM Hepes, 10 mM KCl, 1.5 mM MgCl $_2$ , 1 mM DTT, 0.1% BSA, pH 7.4, containing protease inhibitors), disrupted by sonication and quantified. Samples were resolved in SDS-PAGE using 10% gels, transferred to nitrocellulose membranes, and incubated with the indicated primary antibodies. Rabbit polyclonal antibodies against SCaMC-1, -2, and -3 were used at a dilution of 1:5,000, as previously described (9). Mouse monoclonal Hsp60 antibody (Sigma) and rabbit polyclonal  $\beta$ -ATPase antibody (a kind gift from Dr. J. M. Cuezva, CBMSO) were used at a dilution of 1:10,000. Peroxidase-coupled secondary antibodies were used and proteins were visualized with a chemiluminescence detection kit (ECL, PerkinElmer, Waltham, MA).

**Mitochondria Isolation**—For oxygen consumption measurements and transport assays, liver mitochondria were isolated as previously described (18). Final pellets were resuspended in MSK buffer (75 mM D-mannitol, 25 mM sucrose, 5 mM KH $_2$ PO $_3$ , 20 mM Tris-HCl, 0.5 mM EDTA, 100 mM KCl, and 0.1% BSA fatty acids free, pH 7.4). Muscle mitochondria were extracted from hindlimbs in 100 mM sucrose, 9 mM EDTA, 1 mM EGTA, 100 mM Tris-HCl, 46 mM KCl, pH 7.4, and incubated with protease Nagarse (0.4 mg/ml, 10 min; Sigma) prior to homogenization. For heart mitochondria, the procedure was the same as for muscle, but a different buffer was used (230 mM mannitol, 70 mM sucrose, 1 mM EDTA, 5 mM Tris-HCl, pH 7.4).

**ATP-Mg Transport Assays and AdN Quantification**—Transport assays were performed with 0.5 mg of mitochondria in transport medium (225 mM sucrose, 2 mM KH $_2$ PO $_4$ , 4 mM ATP, 5 mM MgCl $_2$ , 10 mM Tris-HCl, 200 nM ruthenium red (RR), 5 mM succinate, pH 7.4, at 30 °C in the presence of 1 mM EGTA or 20  $\mu\text{M}$  CaCl $_2$  for different lengths of time. The reactions were

stopped by addition of 1.5 volumes of ice-cold transport medium devoid of succinate and supplemented with 1 mM EGTA. Mitochondria were centrifuged at  $14,000 \times g$  for 5 min, and washed twice in the same medium. AdNs were extracted from pellets by incubation with 10% HClO<sub>4</sub> for 60 min. Extracts were centrifuged and neutralized using KOH.

To evaluate the Ca<sup>2+</sup> dependence of the transport, wild type mitochondria were incubated in transport medium with different concentrations of CaCl<sub>2</sub> for 30 s and processed as above. The different Ca<sup>2+</sup> concentrations were prepared using EGTA-Ca<sup>2+</sup> buffers (19). The free Ca<sup>2+</sup> in each medium was determined, in the presence of mitochondria and all reactants with 0.1 μM Calcium Green (Molecular Probes, Invitrogen) using the equation  $[Ca^{2+}] = K_d (F - F_{min}) / (F_{max} - F)$ , where  $F$  is the fluorescence of the medium,  $F_{max}$  and  $F_{min}$  are determined in each case by adding saturating amounts of CaCl<sub>2</sub> ( $F_{max}$ ) or EGTA-Tris, pH 8 ( $F_{min}$ ), and  $K_d$  is 14 μM (20). Fluorescence was measured in a FluoSTAR OPTIMA microplate reader ( $\lambda_{ex}/\lambda_{em} = 506/532$  nm).

Total ATP was quantified using ATP Bioluminescence Assay Kit CLS II (Roche Applied Science) with a FLUOstar OPTIMA microplate reader. ADP was measured by conversion to ATP using 2.5 mM phosphocreatine and 4 units of phosphocreatine kinase. AdN levels were also determined by HPLC. To this end, mitochondrial samples were treated with 10% HClO<sub>4</sub> overnight, neutralized using K<sub>2</sub>CO<sub>3</sub>, kept on ice 10 min, and then at -80 °C for 1 h to allow precipitation of HClO<sub>4</sub>. Extracts were centrifuged and 50 μl of the supernatants were injected for AdN determination (21). To determine the identity of each peak and quantify the amount of the species of interest, standard curves were constructed by plotting peak heights *versus* known concentrations of ATP, ADP, and AMP (22).

**Oxygen Consumption Measurements**—Respiratory rates in isolated mitochondria were determined using a Clark-type oxygen electrode (Hansatech Instruments Ltd., Norfolk, UK) as described previously (23). Measurements were performed at 30 °C in MSK buffer supplemented with 1 mM EGTA unless noted otherwise, using 0.3–0.4 mg of protein. State 4 respiration was assayed in 5 mM glutamate plus malate or 2 μM rotenone plus 5 mM succinate. State 3 was initiated by the addition of 0.5 or 2 mM ADP. To confirm that state 3 was dependent on ATP synthase activity, 6 μM oligomycin was added to the mitochondrial suspension, which resulted in the same respiratory rates as before ADP addition. At the end of each assay, 1–5 μM carbonyl cyanide-4-(trifluoromethoxy)phenylhydrazone (FCCP) or 40–80 μM dinitrophenol (when mitochondria were respiring glutamate plus malate) was added to uncouple mitochondria and obtain maximal respiration, confirming membrane integrity. In both cases, titrations were carried out to obtain maximal respiratory rates. With the exception of experiments using AdN-depleted mitochondria, uncoupled rates were similar to state 3 respiration as previously described (24). Respiratory control ratios were obtained by dividing state 3 by state 4 respiratory rates, which were corrected by subtracting unspecific rates obtained before substrate addition.

In some experiments mitochondria were depleted of AdNs by incubation in MSK with 2 mM tetrasodium pyrophosphate for 5 min at 30 °C (25, 26), centrifuged at  $10,000 \times g$  for 5 min,

and resuspended in fresh MSK. AdN depletion was confirmed by measuring oxygen consumption in the presence of 1 mM EGTA, as depleted mitochondria are unable to stimulate respiration after ADP addition (7). For the filling reactions with ATP-Mg, mitochondria were incubated in MSK devoid of EDTA and supplemented with 200 nM RR and the indicated concentrations of ATP and MgCl<sub>2</sub>, at 30 °C for different lengths of time. The free Ca<sup>2+</sup> concentration of the medium was determined fluorimetrically in the presence of mitochondria, all reactants, and 0.1 μM Calcium Green-5N. Incubations were stopped by introducing the samples in ice, centrifuged ( $10,000 \times g$ , 5 min) and resuspended in the MSK with 1 mM EGTA for oxygen measurements or 10% HClO<sub>4</sub> for AdN quantification.

To assess oxygen consumption in intact attached cells, hepatocytes were plated in XF24 V7 cell culture plates and a Seahorse Bioscience XF24–3 Analyzer (Seahorse Bioscience, Billerica, MA) was used as previously described (27). Before measurements, cell medium was replaced by assay medium (bicarbonate-free DMEM/F-12 (1:1) supplemented with 10 mM sodium lactate and 5 mM glucose) and plates were equilibrated at 37 °C for 60 min. After baseline measurement, one of the following agonists was injected: 0.1 μM glucagon (Sigma), 100 μM phenylephrine (Sigma), or vehicle. Subsequently, all wells were injected sequentially with 6 μM oligomycin, 1 μM FCCP, and 1 μM antimycin A plus 1 μM rotenone to obtain different respiratory parameters.

**Ca<sup>2+</sup> Uptake in Isolated Mitochondria**—The CRC of isolated mitochondria was measured with 0.1 μM Calcium Green-5N as an extramitochondrial Ca<sup>2+</sup> indicator in MSK devoid of EDTA and supplemented with 1 mM MgCl<sub>2</sub> as previously described (28). An Aminco-Bowman fluorimeter provided with temperature control and continuous stirring was used. All experiments were carried out at 30 °C in the presence of respiratory substrates (5 mM succinate + 2 μM rotenone) and in the presence or absence of AdNs (ATP or ADP). After 3–5 min of incubation, mitochondria were challenged with subsequent 10–20 nmol of CaCl<sub>2</sub> additions as indicated in the figure legends, and Ca<sup>2+</sup> uptake into mitochondria was measured as a decrease in fluorescence. The CRC was determined as the total amount of Ca<sup>2+</sup> (in nmol per mg of protein) that the mitochondria are able to take up before starting to release it to the extramitochondrial medium.

**Cytosolic Ca<sup>2+</sup> Measurements**—To monitor cytosolic Ca<sup>2+</sup> signals, hepatocytes growing on coverslips were loaded with 5 μM Fura-2-AM (Molecular Probes, Invitrogen) for 15 min at 37 °C in Ca<sup>2+</sup>-free HCSS medium (120 mM NaCl, 0.8 mM MgCl<sub>2</sub>, 25 mM Hepes, and 5.4 mM KCl) supplemented with 0.05% pluronic acid F-127 (Invitrogen) and washed for 20 min at 37 °C in HCSS with 2 mM CaCl<sub>2</sub>. Coverslips were then mounted in the perfusion chamber of a Zeiss microscope as previously described (29), and fluorescence was imaged ratiometrically at 37 °C using alternate excitation at 340 and 380 nm and a 510-nm emission filter with a Neofluar ×40/0.75 objective. Agonists were added as a bolus. Image acquisition and analysis were performed using Aquacosmos 2.6 software (Hamamatsu Photonics, Hamamatsu, Japan). Ratio signals

## SCaMC-3 Is a Mitochondrial Target of Glucagon

**TABLE 1**

**Glucose and urea levels from wild type and SCaMC-3-KO mice**

Levels were determined in 2–3-month-old mice as indicated under “Experimental Procedures.” Results are expressed as mean  $\pm$  S.E. of 10–15 animals.

	SCaMC-3 WT	SCaMC-3 KO
Glucose (mg/dl)	211.5 $\pm$ 7.8	196.2 $\pm$ 7.0
Urea (md/dl)	31.65 $\pm$ 2.13	24.6 $\pm$ 2.1 <sup>a</sup>

<sup>a</sup>  $p < 0.05$ ; unpaired, two-tailed Student's  $t$  test.

were converted to  $\text{Ca}^{2+}$  concentrations using the calculations described in Ref. 20.

### RESULTS

*SCaMC-3 Is the Only Functional ATP-Mg/P<sub>i</sub> Carrier in Adult Liver*—SCaMC-3-KO and SCaMC-3 heterozygous mice are born in mendelian proportions and have no obvious phenotype, similar to what has been described for SCaMC-2-KO mice (30). Table 1 shows that SCaMC-3-KO mice have normal glucose, but reduced plasma urea levels.

To study whether a compensatory effect is taking place in SCaMC-3-KO animals, we analyzed the protein levels of the other paralogs of the ATP-Mg/P<sub>i</sub> carrier in mitochondria from different adult tissues. The SCaMC-3 signal was found in liver and brain, but not in heart or muscle mitochondria (Fig. 1A), whereas SCaMC-2 and SCaMC-1 were only detected in brain, but not liver. There was no up-regulation of either of these paralogs in mitochondria from SCaMC-3-KO mice. SCaMC-3 levels in late embryonic and early postnatal liver are much lower than in adult liver (Fig. 1B). At these stages, SCaMC-1 showed high levels from E14–E18 until P1, being almost negligible in adult liver, whereas SCaMC-2 expression was not detected (results not shown). Again, no changes in SCaMC-1 levels were detected in embryonic liver mitochondria from SCaMC-3-KO mice.

To study the effect of the lack of SCaMC-3 in mitochondrial respiration, liver mitochondria from wild type and SCaMC-3-KO mice were incubated with 5 mM glutamate plus malate or 2  $\mu\text{M}$  rotenone plus 5 mM succinate in a  $\text{Ca}^{2+}$ -free medium, in the absence or presence of 0.5 mM ADP. Respiratory rates in all conditions, as well as respiratory control ratios, were similar in both genotypes, indicating lack of abnormalities in electron transport chain activity and OXPHOS in SCaMC-3-deficient mitochondria (Fig. 1C).

*SCaMC-3 Catalyzes the Transport of ATP-Mg in Isolated Liver Mitochondria in a  $\text{Ca}^{2+}$ -dependent Manner*—SCaMC-3 has been shown to transport ATP-Mg and ADP in exchange with P<sub>i</sub> in reconstituted proteoliposomes, but the  $\text{Ca}^{2+}$  dependence of this transport has not been characterized (10). We performed transport assays incubating wild type and SCaMC-3-KO liver mitochondria with 4 mM ATP for different lengths of time. Wild type mitochondria show a time-dependent accumulation of ATP, which requires  $\text{Ca}^{2+}$ , as it does not take place when EGTA is present in the medium (Fig. 1D, left panel). No ATP accumulation is observed in SCaMC-3-deficient mitochondria, regardless of whether  $\text{Ca}^{2+}$  is present or not (Fig. 1D, left panel). These results indicate that the transport of ATP-Mg in liver mitochondria is catalyzed by SCaMC-3 by a mechanism that requires  $\text{Ca}^{2+}$ . In another set of experiments the  $\text{Ca}^{2+}$  affinity of ATP-Mg uptake was studied by carrying out assays at

different external  $\text{Ca}^{2+}$  concentrations. An  $S_{0.5}$  for  $\text{Ca}^{2+}$  activation of  $3.3 \pm 0.9 \mu\text{M}$  was obtained (Fig. 1D, right panel). In both experiments RR was present in the medium to prevent  $\text{Ca}^{2+}$  accumulation in the mitochondria.

*CRC Is Impaired in SCaMC-3-deficient Mitochondria*—In the case of SCaMC-1, the mitochondrial ATP-Mg/P<sub>i</sub> transporter found in cancer cells, and the uptake of AdNs through the carrier dramatically increases  $\text{Ca}^{2+}$  retention in mitochondria (28). Therefore, we wondered if the absence of SCaMC-3 affects CRC in mitochondria. To test this possibility, liver mitochondria from wild type and SCaMC-3-KO animals were incubated in the absence of AdNs or in the presence of ATP-Mg or ADP at low (0.2 mM) or physiological (1 mM) concentrations (Fig. 2). In the absence of AdNs, the CRC is similar in both genotypes, and so is the  $\text{Ca}^{2+}$  uptake rate (notice the identical slopes after  $\text{Ca}^{2+}$  addition). Addition of 0.2 mM ADP (or ATP-Mg, not shown) to the medium substantially increases the CRC of mitochondria in both genotypes, most likely by a mechanism mediated by the ANT (31). However, when 1 mM ATP-Mg (or ADP, not shown) is present in the medium, wild type mitochondria show a marked increase in the CRC, with no changes in the initial  $\text{Ca}^{2+}$  uptake rates, whereas SCaMC-3-deficient mitochondria are unable to accumulate higher amounts of  $\text{Ca}^{2+}$ , presumably due to their inability to take up AdNs through SCaMC-3. The existence of a site for regulation of CRC with lower affinity for AdNs than the ANT, and insensitive to carboxyatractyloside has been suggested (32, 33, 34). We have proposed elsewhere (28) that the ATP-Mg/P<sub>i</sub> carrier could be responsible for this site of regulation of the CRC, and hypothesized that calcium retention might be increased in mitochondria by allowing the formation of calcium-phosphate precipitates.

*ATP-Mg or ADP Uptake in AdN-depleted Mitochondria Regulates Coupled Respiration through Extramitochondrial  $\text{Ca}^{2+}$ -dependent SCaMC-3 Activity*—Alterations in the mitochondrial AdN pool have been shown to regulate state 3 respiration in liver mitochondria (25). Incubation with high concentrations of pyrophosphate promotes the efflux of matrix ATP, ADP, and AMP in exchange with external pyrophosphate through the ATP/ADP translocase, leading to a depletion of mitochondrial AdNs (25, 26). In these conditions, state 4 is increased (35), state 3 cannot be induced due to the lack of matrix ATP to be exchanged by external ADP through the ANT, and only the net uptake of ADP or ATP, both of which are transported by the ATP-Mg/P<sub>i</sub> carrier, can restore coupling between electron transport activity and OXPHOS (25).

To study the influence of SCaMC-3-mediated AdN uptake on ADP-stimulated respiration we first depleted mitochondria from AdNs by incubation with pyrophosphate, and then evaluated oxygen consumption. In the presence of extramitochondrial  $\text{Ca}^{2+}$  ( $\sim 3\text{--}4 \mu\text{M}$ ), addition of 2 mM ADP stimulates oligomycin-sensitive respiration in AdN-depleted mitochondria from wild-type but not SCaMC-3-KO mice, whereas no differences were observed in uncoupled respiration between genotypes (Fig. 3A). Matrix  $\text{Ca}^{2+}$  is not required, as the effect is observed in the presence of 200 nM RR to inhibit  $\text{Ca}^{2+}$  accumulation by the mitochondria. However, extramitochondrial  $\text{Ca}^{2+}$  is strictly required for the stimulation, as addition of 2 mM ADP

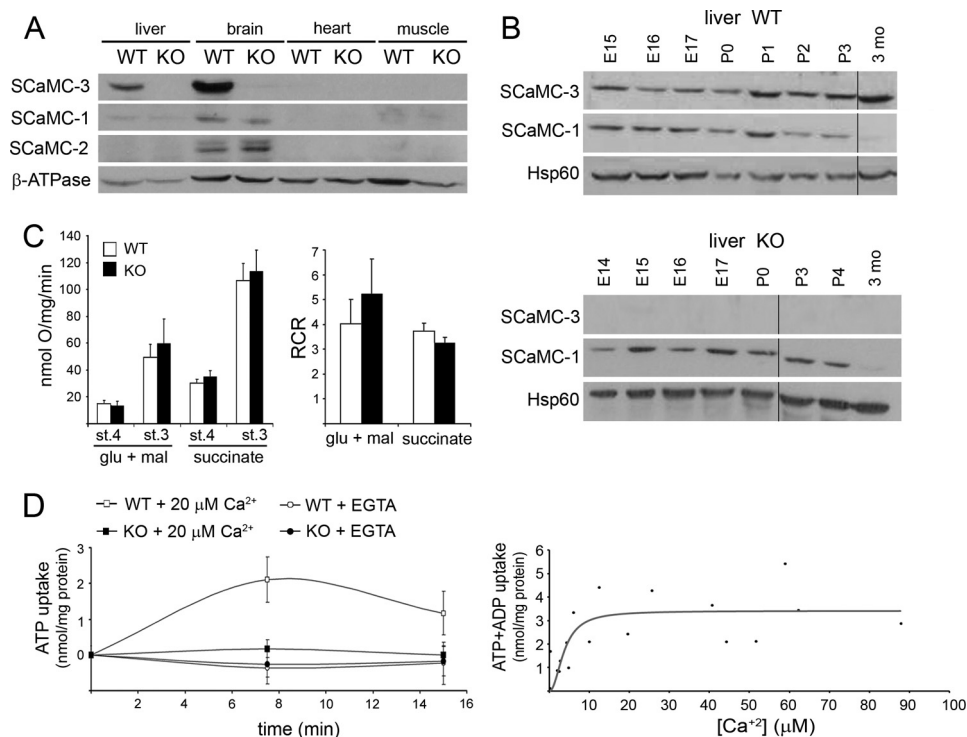


**FIGURE 1. SCaMC-3 is the main functional  $\text{Ca}^{2+}$ -dependent ATP-Mg/ $\text{P}_i$  carrier in adult liver.** *A*, expression levels of the main SCaMC paralogs were analyzed by Western blot in isolated mitochondria using different tissues from wild type (WT) and SCaMC-3-KO (KO) mice.  $\beta$ -ATPase was used as loading control. *B*, Western blot analysis of liver extracts from embryos (E14–E17), postnatal (P0–P4), and 3-month-old mice (3 mo) from wild type and SCaMC-3-KO mice. Antibodies against SCaMC-1 and SCaMC-3, as well as Hsp60 as loading control, were used. Absence of SCaMC-3 did not induce up-regulation of other ATP-Mg/ $\text{P}_i$  paralogs. *C*, respiratory rates were measured in isolated liver mitochondria from wild type and SCaMC-3-KO mice using substrates for complex I (*glu + mal*) or complex II (*succinate*) in the presence (state 3, *st. 3*) or absence (state 4, *st. 4*) of 0.5 mM ADP. Respiratory control ratios (state 3/state 4; *RCR*) using substrates for complex I or complex II are also shown. Results are expressed as mean  $\pm$  S.E. of 8 (complex I) and 22 (complex II) independent experiments. *D*, SCaMC-3 transports ATP-Mg in a  $\text{Ca}^{2+}$ -dependent way. *Left panel* shows ATP uptake in isolated liver mitochondria from wild type and SCaMC-3-KO mice in the presence or absence of  $\text{Ca}^{2+}$ . Mitochondria were incubated at 30 °C in the presence of 4 mM ATP, 5 mM  $\text{Mg}^{2+}$ , and 200 nM RR, with 20  $\mu\text{M}$   $\text{Ca}^{2+}$  or 1 mM EGTA in the medium, and mitochondrial ATP levels were determined. Results are expressed as mean  $\pm$  S.E. of 3 independent experiments. In the *right panel*, kinetics of  $\text{Ca}^{2+}$  activation of ATP uptake in SCaMC-3 wild type liver mitochondria are shown. Data obtained were fitted by nonlinear regression to the following equation:  $V = V_0 + [(V_{\text{max}} - V_0) \times [\text{Ca}^{2+}]^n] / (S_{0.5}^n + [\text{Ca}^{2+}]^n)$  (where  $V$  is transport activity at each  $[\text{Ca}^{2+}]$ ,  $V_0$  is the basal transport rate at 0  $[\text{Ca}^{2+}]$  (*i.e.* below the Calcium-Green detection limit),  $V_{\text{max}}$  is the maximal activity,  $n$  is the Hill index, and  $S_{0.5}$  is the  $\text{Ca}^{2+}$  concentration that generates half-maximal transport activity) using Sigma Plot version 9. Pooled data from 4 independent experiments are shown.

in the presence of 1 mM EDTA and 1 mM EGTA fails to induce state 3 respiration (Fig. 3*B*). In this last condition (*i.e.* AdN-depleted mitochondria in  $\text{Ca}^{2+}$ -free medium), state 4 respiratory rates are increased as previously described (35), both in wild type and SCaMC-3-deficient mitochondria. However, stimulation of the respiration can still be achieved, as mitochondria increase their respiratory rates in response to FCCP (Fig. 3*B*). Taken together, these results indicate that matrix AdNs are required to achieve state 3 but not fully uncoupled respiration.

Although the ATP-Mg/ $\text{P}_i$  carrier can transport both ATP-Mg and ADP in isolated mitochondria and reconstituted liposomes, it has been shown that ATP-Mg is the preferred substrate under normal energized conditions, as the cytosolic ATP concentration exceeds that of ADP (36). To study the respiratory effect of ATP-Mg uptake in AdN-depleted mitochondria, these were incubated at 30 °C in the presence of 2 mM ATP, 5 mM  $\text{MgCl}_2$ , and 200 nM RR for different lengths of time, and then the ADP-response to oxygen consumption in the presence of 1 mM EGTA was evaluated. After 1 min of incubation, wild type but not SCaMC-3-KO mitochondria showed a slight nonsignificant decrease in state 4 respiratory rates (Fig. 4*A*, *state 4*) and an increase in state 3 respiration, which was

maximum after 2 min (Fig. 4*A*, *state 3*). This is reflected in a gradual increase in respiratory control ratios, but not in uncoupled respiration (Fig. 4*A*, *uncoupled*), which occurs in wild type but not SCaMC-3 deficient mitochondria (Fig. 4*A*, *RCR*). These results indicate that extramitochondrial  $\text{Ca}^{2+}$ -dependent AdN uptake through SCaMC-3 couples electron transport chain activity and OXPHOS in isolated mitochondria after AdN depletion.

To study the consequences of ATP-Mg uptake in normal, nondepleted organelles, liver mitochondria from wild type and SCaMC-3-KO mice were incubated with 10 mM ATP and 10 mM  $\text{Mg}^{2+}$  in the presence of 5 mM succinate and 200 nM RR, washed, and assayed for ADP + ATP content and respiration. As observed in Fig. 3*B*, this resulted in a rapid increase in matrix ADP + ATP in both genotypes, but much lower in SCaMC-3-KO than in wild type mitochondria. These results emphasize the role of SCaMC-3 in AdN “superfilling” and suggest that under these conditions, other transport processes (including pyrophosphate<sub>in</sub>/AdN<sub>out</sub> exchange on ANT) contribute to refilling. In contrast with the results on AdN-depleted mitochondria, despite the large increase in the AdN pool, states 3 and 4 and uncoupled respiratory rates were unchanged regardless of the presence of SCaMC-3 (Fig. 4*B*).

## SCaMC-3 Is a Mitochondrial Target of Glucagon

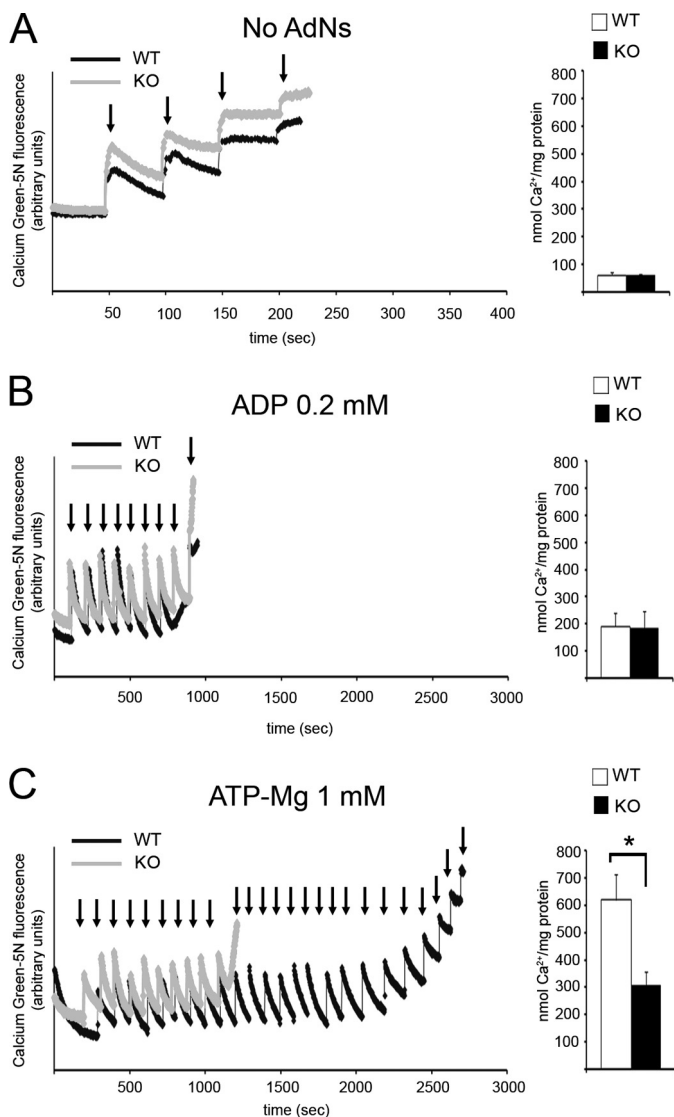


**FIGURE 2. SCaMC-3 mediates the increase in Ca<sup>2+</sup> retention capacity in liver mitochondria.** Mitochondrial Ca<sup>2+</sup> uptake was monitored using the fluorescent indicator Calcium Green-5N in the absence of AdNs in the medium (A) or in the presence of 0.2 mM ADP (B) or 1 mM ATP-Mg (C). Arrows indicate additions of 10 (A) or 20 (B and C) nmol of CaCl<sub>2</sub>. Quantification of total Ca<sup>2+</sup> retained by mitochondria in each case is shown on the right side of each panel. Results are expressed as mean ± S.E. of 3–5 independent experiments (\*, *p* < 0.05; unpaired, two-tailed Student's *t* test).

*Glucagon and Phenylephrine Exert Their Effects on Mitochondrial Respiration through SCaMC-3*—Having shown that SCaMC-3 is able to induce an increase in liver mitochondrial AdN content and coupled respiration that does not occur in SCaMC-3-KO mitochondria, we next studied whether this mechanism is responsible for glucagon stimulation of mitochondrial respiration in hepatocytes (2). The stimulation by glucagon of AdN uptake in liver mitochondria is dependent on the generation of a Ca<sup>2+</sup> signal (4). Similarly, Ca<sup>2+</sup>-mobilizing agents like phenylephrine have been shown to increase the mitochondrial AdN content in hepatocytes (37). In each case, the nature of the Ca<sup>2+</sup> signals evoked is different and both agonists are known to be synergistically potentiated (38). Fig. 4A shows the effect of these agonists on cytosolic Ca<sup>2+</sup> in isolated hepatocytes using fura2-AM. Transients elicited by 0.1 μM glu-

cagon show a delayed onset of about 2 min (Fig. 5A), whereas addition of 100 μM phenylephrine induces an immediate increase in cytosolic Ca<sup>2+</sup> (Fig. 5A). In both cases, cells that show spontaneous oscillatory behavior before the addition increase their oscillation frequency, whereas most of the non-oscillatory cells start to oscillate (data not shown). No differences were observed between genotypes.

We next studied the effect of glucagon and phenylephrine on the oxygen consumption rate (OCR) of intact primary hepatocytes using a Seahorse Extracellular Flux Analyzer. Experiments were performed using the layout represented in Fig. 5B. Both genotypes showed similar basal rates normalized by protein content (1.9 ± 0.7 nmol/min/mg in wild type cells *versus* 1.7 ± 0.6 nmol/min/mg in SCaMC-3-deficient cells). Both glucagon and phenylephrine cause an immediate stimulation of the OCR in wild type cells of about 20% with respect to vehicle, which is significantly lower (about 5%) in SCaMC-3-KO hepatocytes (Fig. 5, C and D, agonist-induced stimulation). In wild type cells most of this stimulation is due to an increase in coupled respiration (*i.e.* oligomycin sensitive), particularly in the case of glucagon, whereas neither of the two agonists increase coupled respiration in SCaMC-3-KO cells (Fig. 5D, coupled respiration). Glucagon also induces an increase of about 20% in the maximal respiratory capacity (*i.e.* FCCP-stimulated respiration) in hepatocytes from wild type mice, but not in those from SCaMC-3-KO mice (Fig. 5, C and D, maximal respiratory capacity). Phenylephrine effects on maximal respiratory capacity and coupled respiration followed the same trend but did not reach statistical significance. Neither glucagon nor phenylephrine have a significant effect on proton leak values in any of the genotypes (Fig. 5D, *proton leak*). Taken together, these results show that glucagon and phenylephrine induce a rapid increase in mitochondrial respiration from intact primary hepatocytes (particularly coupled respiration) and that this effect is largely lost in hepatocytes that lack SCaMC-3.

*AdN Uptake, CRC, and Stimulation of Respiration in Mitochondria after Glucagon Treatment in Vivo Is Mediated by SCaMC-3*—To verify that the effects found in isolated mitochondria and primary hepatocytes are also present in the intact animal, we next studied the effect of *in vivo* administration of glucagon, which has been shown to promote uptake of AdNs and to stimulate respiration in liver mitochondria (4, 39, 40). To study the involvement of SCaMC-3 in this hormonal response, we injected glucagon intraperitoneally in wild type and SCaMC-3-KO mice and sacrificed them 15 min later to analyze liver mitochondrial AdN content and respiratory rates. Fig. 5A shows that liver mitochondria from wild type mice undergo a striking increase of about 50% in their AdN levels in response to glucagon treatment, whereas the levels in SCaMC-3-KO mitochondria remain unaffected by the treatment. The increase is not restricted to a particular AdN form, but rather affects all three: AMP, ADP, and ATP (Fig. 6A, right panel). Interestingly, under control (vehicle) conditions, ATP levels were found to be lower in SCaMC-3-KO than in wild type mitochondria. Although extraction procedures do not warrant that these concentrations correspond to real levels of the three AdNs *in vivo*, they suggest that SCaMC-3 deficiency might involve a decrease in mitochondrial ATP levels. In fact, mouse embryonic fibro-

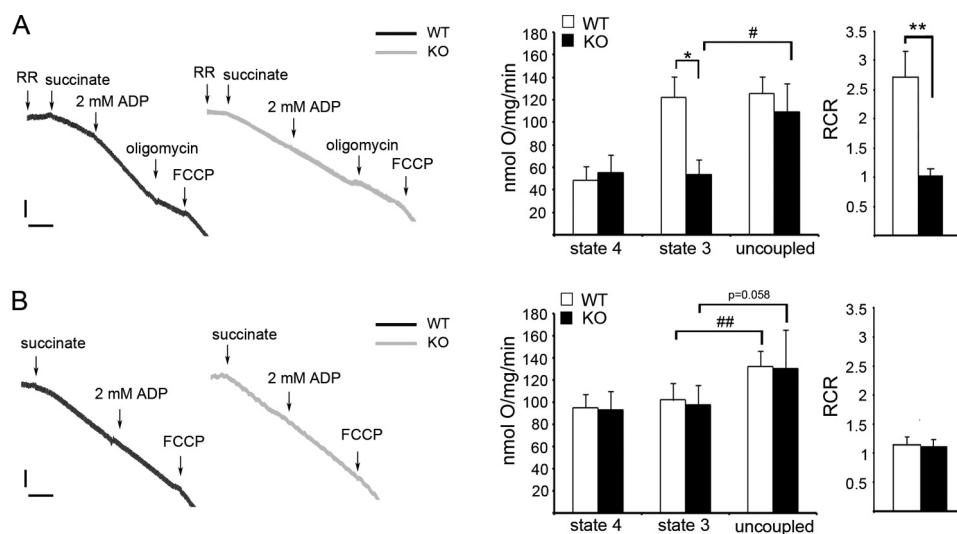


**FIGURE 3. Addition of ADP to AdN-depleted mitochondria stimulates respiration through SCaMC-3.** Representative electrode traces and respiratory rates of AdN-depleted liver mitochondria from wild type (WT) and SCaMC-3-KO mice respiring on succinate and stimulated with 2 mM ADP in the presence of Ca<sup>2+</sup> (A) or in the presence of 1 mM EGTA and 1 mM EDTA (B). State 3 respiratory rate and respiratory control ratio (RCR) are only stimulated in wild type liver mitochondria in the presence of extramitochondrial Ca<sup>2+</sup>. Results are expressed as mean  $\pm$  S.E. of 3–5 independent experiments. \*,  $p < 0.05$ ; \*\*,  $p < 0.01$ ; WT versus KO two-tailed, unpaired Student's *t* test; #,  $p < 0.05$ ; ##,  $p < 0.01$ ; state 3 versus uncoupled two-tailed, paired Student's *t* test. Scale bars: 10 nmol at O (vertical) and 1 min (horizontal).

blast derived from SCaMC-2-KO mice show lower cellular ATP levels (30).

In the liver of fed rats, glucagon administration also leads to a rapid increase in the CRC (41) and Ca<sup>2+</sup> content (42) of rat liver mitochondria. The increase in mitochondrial Ca<sup>2+</sup> plays a role in activation of mitochondrial dehydrogenases and regulation of respiration (43). Having found that SCaMC-3 is required to increase CRC in response to AdN accumulation, we evaluated whether SCaMC-3 may also be involved in increasing the CRC of mitochondria in response to glucagon. Fig. 6B shows that glucagon treatment results in a prominent increase in CRC in liver mitochondria from wild type mice (compare Fig. 2A with 6B), which is essentially blunted in SCaMC-3-deficient mitochondria. Fig. 6C also shows that glucagon administration *in vivo* stimulates state 4, state 3, and uncoupled respiration in liver mitochondria using respiratory substrates of complex I or II, but fails to do so in SCaMC-3-deficient mitochondria. As previously described (44, 45), respiratory rates using TMPD plus ascorbate as substrates were not affected by glucagon administration, nor was complex IV activity (results not shown). Therefore, the lack of SCaMC-3 blocks the responses of liver mitochondria to glucagon *in vivo*, preventing AdN accumulation, CRC increase, and stimulation of respiration.

## DISCUSSION

We have shown that SCaMC-3 is the main mitochondrial ATP-Mg/P<sub>i</sub> transporter in adult liver from mice. We find that SCaMC-3 has an S<sub>0.5</sub> for Ca<sup>2+</sup> activation of  $3.3 \pm 0.9 \mu\text{M}$ , a value substantially lower than that of SCaMC-1 ( $12.7 \pm 5.3 \mu\text{M}$ ) (28) or the yeast ATP-Mg/P<sub>i</sub> carrier, Sal1p ( $15.0 \pm 1.1 \mu\text{M}$ ) (19). Ca<sup>2+</sup> increases the V<sub>max</sub> of these carriers with no changes in the K<sub>m</sub> for the substrates, which are similar for both ATP-Mg and ADP in all cases, ranging from 0.2 to 0.5 mM (10).

Previous studies have shown that the filling of the mitochondria with cytosolic AdNs during the first postnatal hours is

important in liver adaptation to an aerobic environment (46). However, despite the fact that SCaMC-3 is the main paralog of the carrier in adult liver, SCaMC-3-KO mice are born in mendelian proportions, do not show obvious developmental defects, and lack compensatory effects caused by up-regulation of other mitochondrial transporters of ATP-Mg/P<sub>i</sub>. This may be explained by our finding that SCaMC-1 and SCaMC-3 are both co-expressed in the embryonic and early postnatal liver, and therefore, SCaMC-1 may compensate for the lack of SCaMC-3 during postnatal development.

Glucagon is known to exert multiple effects on liver mitochondria including the increase in AdN content, respiration, and CRC, as well as enhanced synthesis of citrulline and pyruvate carboxylation (43). Regarding the first of these effects, our results have clarified how glucagon and phenylephrine cause an increase in mitochondrial AdN content. To date, two hypotheses had been proposed: in the first, Davidson and Halestrap (6) suggested that Ca<sup>2+</sup> entry in the mitochondria could inhibit matrix pyrophosphatase, leading to an increase in matrix pyrophosphate that would then be exchanged by cytosolic AdNs through the ANT. The second mechanism, put forward by Aprille and co-workers (2, 7), involves Ca<sup>2+</sup> activation of the ATP-Mg/P<sub>i</sub> carrier. Our data clearly support this latter hypothesis, showing that the increase in liver mitochondrial AdNs in response to glucagon does not take place in the absence of SCaMC-3 (Fig. 6B), which is the only functional ATP-Mg/P<sub>i</sub> carrier in adult liver (Fig. 1).

Moreover, the present work also sheds light on the effect of glucagon on mitochondrial CRC and its relationship with mitochondrial AdN content. In agreement with previous findings related to SCaMC-1 (28) our results show that Ca<sup>2+</sup> activation of AdN uptake through SCaMC-3 causes an accumulation of matrix AdNs, which increases mitochondrial CRC. This may be due to the formation of Ca<sup>2+</sup>-phosphate precipitates, as this

## SCaMC-3 Is a Mitochondrial Target of Glucagon

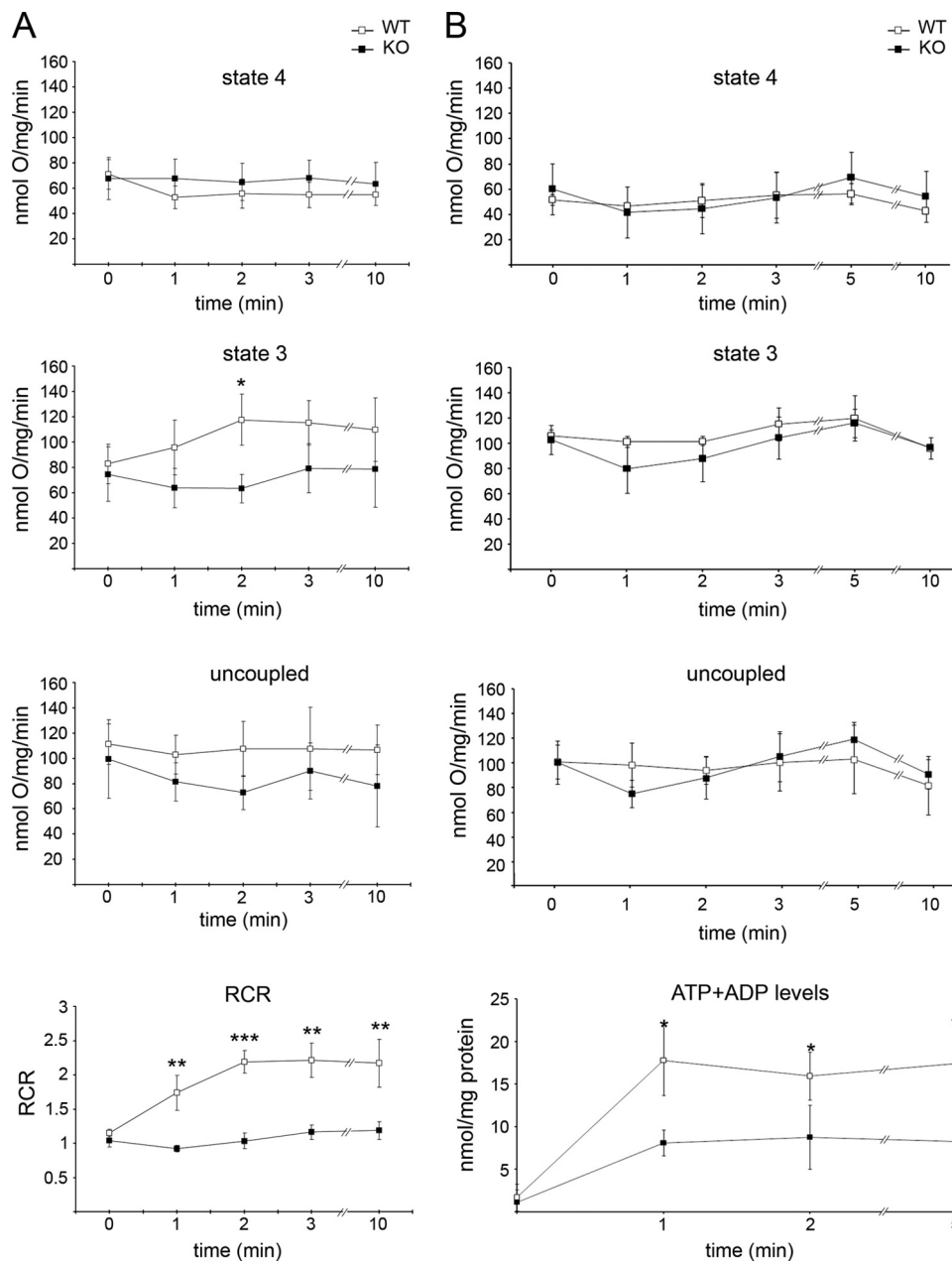


**FIGURE 4. Respiration in mitochondria loaded with AdNs.** *A*, wild type (WT) and SCaMC-3-KO (KO) mitochondria were depleted from AdNs and incubated at 30 °C in the presence of 200 nM RR, 2 mM ATP, and 5 mM MgCl<sub>2</sub> for different lengths of time before monitoring state 4, state 3, and uncoupled respiratory rates in the presence of 2 μM rotenone plus 5 mM succinate. Respiratory control ratios (RCR) are also shown. The maximal increase of state 3 respiratory rate is observed in wild type cells after 2 min of incubation. Results are expressed as mean ± S.E. of 5 independent experiments (\*,  $p < 0.05$ ; \*\*,  $p < 0.01$ ; two-tailed, unpaired Student's *t* test). *B*, nondepleted wild type and SCaMC-3-KO mitochondria were incubated at 30 °C in the presence of 200 nM RR, 10 mM ATP, 10 mM MgCl<sub>2</sub>, and 20 μM CaCl<sub>2</sub> at different times before monitoring state 4, state 3, and uncoupled respiratory rates as in *A*. To correct for residual AdNs in the medium, state 4 was that obtained after the addition of oligomycin. In parallel, mitochondrial levels of ATP + ADP were also determined (bottom panel). Results are expressed as mean ± S.E. of 3–5 independent experiments (\*,  $p < 0.05$ , two-tailed, unpaired Student's *t* test).

process requires AdNs (47). Moreover, SCaMC-3 deficiency prevents the increase in CRC caused by glucagon administration, showing that this effect of glucagon is mediated by SCaMC-3.

We have shown that SCaMC-3 can regulate oxidative phosphorylation under certain conditions. We report a striking effect of SCaMC-3-mediated Ca<sup>2+</sup>-dependent uptake of ADP or ATP-Mg in liver mitochondria, which effectively couples respiration and OXPHOS, most likely by increasing the total mitochondrial AdN pool. Previous studies have shown a bipha-

sic correlation between mitochondrial AdN content and respiratory functions, which is especially steep when matrix AdN levels are below 4 nmol/mg of protein, but becomes more moderate at higher concentrations (25). Our own results confirm this dependence on the size of the AdN pool of state 3 respiration at relatively low matrix AdN levels (Fig. 4A) but not at higher AdN levels (Fig. 4B). It is important to note that RR was present in these experiments, ruling out an effect of matrix Ca<sup>2+</sup>. Therefore, it is likely that the stimulation of respiration observed by progressively increasing the AdN content is due to



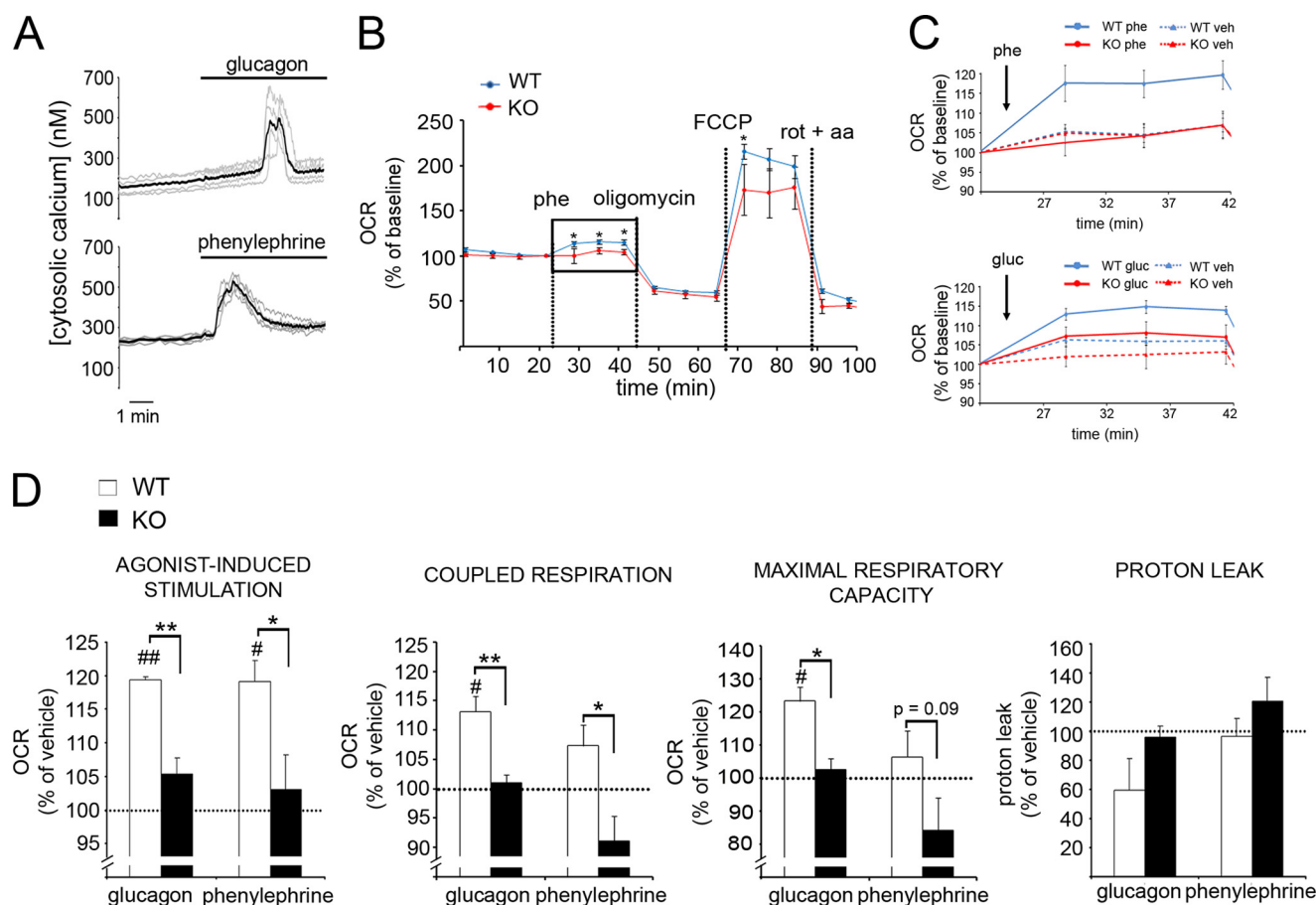


**FIGURE 5. Effects of glucagon and phenylephrine on cytosolic  $\text{Ca}^{2+}$  signals and respiratory parameters in primary hepatocytes from wild type and SCaMC-3-KO animals.** *A*, representative traces corresponding to cytoplasmic  $\text{Ca}^{2+}$  concentration in primary wild type hepatocytes in response to  $0.1 \mu\text{M}$  glucagon and  $100 \mu\text{M}$  phenylephrine addition. Light gray traces correspond to individual cells, whereas the average is represented by a black trace. In both genotypes phenylephrine caused an immediate  $\text{Ca}^{2+}$  peak, whereas the effect of glucagon was detectable 2 min after its addition. The  $\text{Ca}^{2+}$  signals evoked by both agonists were identical in SCaMC-3-KO cells. *B*, a representative experiment of OCR in primary hepatocytes from wild type and SCaMC-3-KO and the response to phenylephrine is shown. OCR is expressed as the rate at each point with respect to the basal rate at the time of addition of the agonist. Where indicated,  $100 \mu\text{M}$  phenylephrine,  $6 \mu\text{M}$  oligomycin,  $1 \mu\text{M}$  FCCP, and  $1 \mu\text{M}$  rotenone plus  $1 \mu\text{M}$  antimycin A (*rot + AntA*) were injected. *C*, OCR responses to phenylephrine ( $100 \mu\text{M}$ ) and glucagon ( $0.1 \mu\text{M}$ ) and the corresponding vehicle in hepatocytes from WT and SCaMC-3 KO mice. Data correspond to representative experiments. *D*, respiratory parameters after treatment with  $0.1 \mu\text{M}$  glucagon or  $100 \mu\text{M}$  phenylephrine with respect to vehicle in wild type and SCaMC-3-KO hepatocytes. Nonmitochondrial respiration (the lowest value remaining after rotenone plus antimycin A addition) was subtracted from all measurements after confirming that at longer times respiration was not further decreased. Respiratory parameters were calculated as the average of three consecutive measurements after each addition (agonist, oligomycin, and FCCP). The stimulations of glucagon and phenylephrine and maximal respiratory capacity were calculated as the percentage of respiration after oligomycin or FCCP addition with respect to basal respiration. Coupled respiration is the percentage of respiration in the presence of agonist sensitive to oligomycin inhibition. Proton leak was calculated as the difference between oligomycin-sensitive and nonmitochondrial respiration. Results are expressed as mean  $\pm$  S.E. of 3 independent experiments with four replicates each (\*,  $p < 0.05$ ; \*\*,  $p < 0.01$ ; unpaired, two-tailed Student's *t* test, WT versus KO; #,  $p < 0.01$  ##,  $p < 0.001$  two-tailed Student's *t* test, WT versus vehicle).

direct mass-action ratio effects of ADP and ATP on the ATP synthase and/or the ANT. This stimulation may be important in situations where mitochondrial AdN levels are low, like in newborn liver and ischemic mitochondria, where even small changes in the mitochondrial AdN content may bring about significant changes in respiratory rates coupled to ATP synthesis, as previously suggested by Aprille (5).

However, the mechanism whereby an increase in mitochondrial AdN content will increase coupled and maximal respiration in the healthy adult liver, as occurs after treatment with glucagon, is unclear. As mentioned above, our results show that beyond a certain threshold, further accumulation of adenine nucleotides does not affect respiration rates. This contrasts sharply with the consequences of the stimulation by glucagon in intact hepatocytes and *in vivo*, where an increase in matrix AdN content is associated with an increase both in coupled and

maximal uncoupled respiration, and a pronounced increase in respiratory capacity in isolated mitochondria, all of which require the presence of SCaMC-3.

The stimulation of respiration by glucagon has been the subject of a great amount of work during the 70s and 80s, although the site of action of the hormone remains unknown. The enhancement of oxygen consumption is observed when the electron transport chain is fuelled with substrates of complex I or complex II, but not when TMPD plus ascorbate are used instead (44). It has been concluded that glucagon-induced activation of respiration involves increases in electron flow into the ubiquinone pool and within complex III (48, 49). The mechanism proposed for such stimulation is a moderate increase in matrix volume caused by the uptake of  $\text{Ca}^{2+}$  into the mitochondria following glucagon-induced cytosolic  $\text{Ca}^{2+}$  signals. By inhibiting mitochondrial pyrophosphatase activity, matrix

## SCaMC-3 Is a Mitochondrial Target of Glucagon

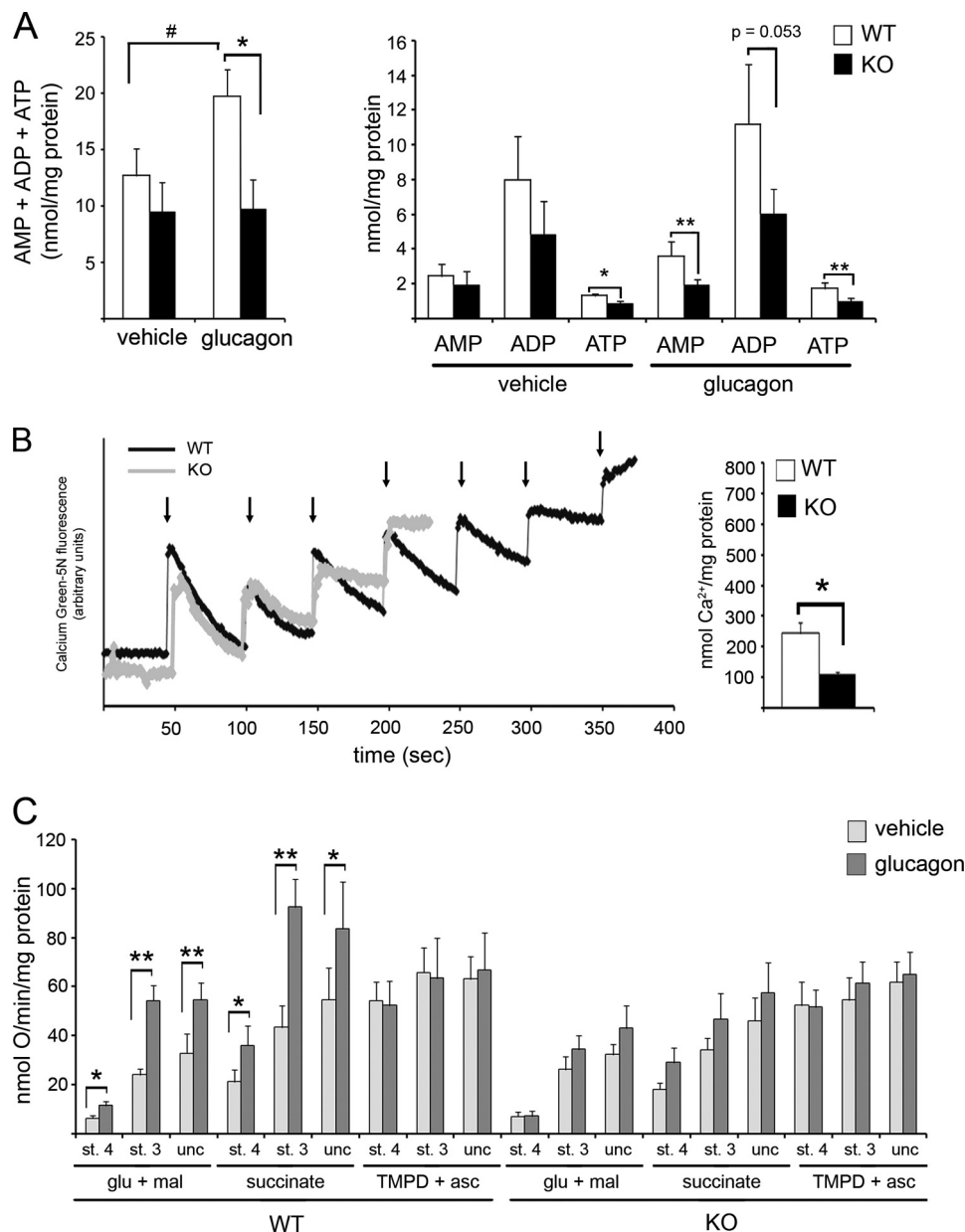


**FIGURE 6. SCaMC-3 mediates glucagon-stimulated mitochondrial uptake of AdNs and increase in CRC and respiratory activity *in vivo*.** Following *in vivo* administration of glucagon (2 mg/kg) or vehicle, liver mitochondria from wild type and SCaMC-3-KO mice were rapidly isolated and different mitochondrial parameters were evaluated. **A**, matrix AdN content, measured by HPLC. *Left panel* shows total AdNs, whereas the *right panel* shows the levels of the different AdNs. Results are expressed as mean  $\pm$  S.E. of 3–5 independent experiments (\*,  $p < 0.05$ ; WT versus KO, two-tailed, unpaired Student's *t* test; #,  $p < 0.05$ ; WT vehicle versus WT glucagon, one-tailed, unpaired Student's *t* test). **B**, Ca<sup>2+</sup> retention in isolated mitochondria. *Left panel* shows a representative experiment, with arrows corresponding to 10 nmol of CaCl<sub>2</sub> additions. In the *right panel*, CRC is shown. Results are expressed as mean  $\pm$  S.E. of 3 independent experiments (\*,  $p < 0.05$ ; WT versus KO, two-tailed, unpaired Student's *t* test). **C**, state 4 (st. 4), state 3 (st. 3), and uncoupled (unc) respiratory rates using different substrates. Results are expressed as mean  $\pm$  S.E. of 6 independent experiments (\*,  $p < 0.05$ ; vehicle versus glucagon, two-tailed paired Student's *t* test; \*\*,  $p < 0.01$ ; vehicle versus glucagon, two-tailed paired Student's *t* test).

Ca<sup>2+</sup> would cause an increase in pyrophosphate, in addition to induce a K<sup>+</sup> influx into the mitochondria through a K<sup>+</sup> uniporter whose nature is still debated (50). Matrix Ca<sup>2+</sup> itself may control coupled respiration through matrix Ca<sup>2+</sup> activation of ATP synthase (51).

Therefore, it is possible that the increase in mitochondrial CRC conferred by SCaMC-3 could explain the role of SCaMC-3 in glucagon signaling. By allowing Ca<sup>2+</sup> accumulation in mitochondria *in vivo*, SCaMC-3 might be permissive for K<sup>+</sup> entry, pyrophosphate accumulation in mitochondria, and/or other

glucagon targets, which would in turn modulate the increase in matrix volume and stimulate respiration (43).

A reduced CRC in mitochondria could also explain the different responses to glucagon and phenylephrine in SCaMC-3-deficient hepatocytes. Whereas glucagon does not affect coupled or maximal respiration, phenylephrine tends to lower both parameters in these cells. Phenylephrine-induced Ca<sup>2+</sup> signals arise faster (Fig. 5A), are more persistent in time (52), and give rise to larger changes in light scattering in isolated hepatocytes than those of glucagon (49, 53), indicative of a higher require-

ment for CRC in mitochondria than for glucagon. It is feasible that under these conditions, impaired  $\text{Ca}^{2+}$  retention in SCaMC-3-deficient mitochondria may hamper the respiratory response to phenylephrine.

Interestingly, the present study provides indications that SCaMC-3 is also required for the operation of the urea cycle. Glucagon increases urea synthesis by activation of carbamoyl-phosphate synthetase, a limiting step in this process (49), and it has been proposed that increased ATP synthesis in mitochondria may account for this effect of glucagon (5). Although we have not measured blood ammonia, the drop in blood serum urea levels found in SCaMC-3 KO mice (Table 1) could be due to a limited function of the urea cycle in SCaMC-3 deficiency, which in turn may be associated with a decreased content of mitochondrial adenine nucleotides in response to glucagon.

*Acknowledgments*—We thank Professor June Aprille for critical reading of the manuscript and valuable comments. We also thank Isabel Manso, Alejandro Arandilla, and Barbara Sesé for excellent technical support.

## REFERENCES

- Ramnanan, C. J., Edgerton, D. S., Kraft G., and Cherrington, A. D. (2011) Physiologic action of glucagon on liver glucose metabolism. *Diabetes Obes. Metab.* **13**, 118–125
- Aprille, J. R., Nosek, M. T., and Brennan, W. A., Jr. (1982) Adenine nucleotide content of liver mitochondria increases after glucagon treatment of rats or isolated hepatocytes. *Biochem. Biophys. Res. Commun.* **108**, 834–839
- Barritt, G. J., Chen, J., and Rychkov, G. Y. (2008)  $\text{Ca}^{2+}$ -permeable channels in the hepatocyte plasma membrane and their roles in hepatocyte physiology. *Biochim. Biophys. Acta* **1783**, 651–672
- Haynes, R. C., Jr., Picking, R. A., and Zaks, W. J. (1986) Control of mitochondrial content of adenine nucleotides by submicromolar calcium concentrations and its relationship to hormonal effects. *J. Biol. Chem.* **261**, 16121–16125
- Aprille, J. R. (1988) Regulation of the mitochondrial adenine nucleotide pool size in liver. Mechanism and metabolic role. *FASEB J.* **2**, 2547–2556
- Davidson, A. M., and Halestrap, A. P. (1988) Inorganic pyrophosphate is located primarily in the mitochondria of the hepatocyte and increases in parallel with the decrease in light-scattering induced by gluconeogenic hormones, butyrate and ionophore A23187. *Biochem. J.* **254**, 379–384
- Nosek, M. T., Dransfield, D. T., and Aprille, J. R. (1990) Calcium stimulates ATP-Mg/ $\text{P}_i$  carrier activity in rat liver mitochondria. *J. Biol. Chem.* **265**, 8444–8450
- Aprille, J. R., and Asimakis, G. K. (1980) Postnatal development of rat liver mitochondria. State 3 respiration, adenine nucleotide translocase activity, and the net accumulation of adenine nucleotides. *Arch. Biochem. Biophys.* **201**, 564–575
- del Arco, A., and Satrústegui, J. (2004) Identification of a novel human subfamily of mitochondrial carriers with calcium-binding domains. *J. Biol. Chem.* **279**, 24701–24713
- Fiermonte, G., De Leonardi, F., Todisco, S., Palmieri, L., Lasorsa, F. M., and Palmieri, F. (2004) Identification of the mitochondrial ATP-Mg/ $\text{P}_i$  transporter. Bacterial expression, reconstitution, functional characterization, and tissue distribution. *J. Biol. Chem.* **279**, 30722–30730
- Satrústegui, J., Pardo, B., and Del Arco, A. (2007) Mitochondrial transporters as novel targets for intracellular calcium signaling. *Physiol. Rev.* **87**, 29–67
- Haitina, T., Lindblom, J., Renström, T., and Fredriksson, R. (2006) Fourteen novel human members of mitochondrial solute carrier family 25 (SLC25) widely expressed in the central nervous system. *Genomics* **88**, 779–790
- Traba, J., Satrústegui, J., and del Arco, A. (2009) Characterization of SCaMC-3-like/slc25a41, a novel calcium-independent mitochondrial ATP-Mg/ $\text{P}_i$  carrier. *Biochem. J.* **418**, 125–133
- Amigo, I., Traba, J., Satrústegui, J., and del Arco, A. (2012) SCaMC-1 like a member of the mitochondrial carrier (MC) family preferentially expressed in testis and localized in mitochondria and chromatoid body. *PLoS ONE* **7**, e40470
- Traba, J., Satrústegui, J., and del Arco, A. (2011) Adenine nucleotide transporters in organelles. Novel genes and functions. *Cell. Mol. Life Sci.* **68**, 1183–1206
- Aprille, J. R. (1993) Mechanism and regulation of the mitochondrial ATP-Mg/ $\text{P}_i$  carrier. *J. Bioenerg. Biomembr.* **25**, 473–481
- Kao, C. Y., Factor, V. M., and Thorgeirsson, S. S. (1996) Reduced growth capacity of hepatocytes from c-myc and c-myc/TGF- $\alpha$  transgenic mice in primary culture. *Biochem. Biophys. Res. Commun.* **222**, 64–70
- Contreras, L., and Satrústegui, J. (2009) Calcium signaling in brain mitochondria. Interplay of malate aspartate NADH shuttle and calcium uniporter/mitochondrial dehydrogenase pathways. *J. Biol. Chem.* **284**, 7091–7099
- Traba, J., Froeschauer, E. M., Wiesenberger, G., Satrústegui, J., and Del Arco, A. (2008) Yeast mitochondria import ATP through the calcium-dependent ATP-Mg/ $\text{P}_i$  carrier Sal1p, and are ATP consumers during aerobic growth in glucose. *Mol. Microbiol.* **69**, 570–585
- Gryniewicz, G., Poenie, M., and Tsien, R. Y. (1985) A new generation of  $\text{Ca}^{2+}$  indicators with greatly improved fluorescence properties. *J. Biol. Chem.* **260**, 3440–3450
- González-Barroso, M. M., Anedda, A., Gallardo-Vara, E., Redondo-Horcajo, M., Rodríguez-Sánchez, L., and Rial, E. (2012) Fatty acids revert the inhibition of respiration caused by the antidiabetic drug metformin to facilitate their mitochondrial  $\beta$ -oxidation. *Biochim. Biophys. Acta* **1817**, 1768–1775
- Vives-Bauza, C., Yang, L., and Manfredi, G. (2007) Assay of mitochondrial ATP synthesis in animal cells and tissues. *Methods Cell Biol.* **80**, 155–171
- Jalil, M. A., Begum, L., Contreras, L., Pardo, B., Iijima, M., Li, M. X., Ramos, M., Marmol, P., Horiuchi, M., Shimotsu, K., Nakagawa, S., Okubo, A., Sameshima, M., Isashiki, Y., Del Arco, A., Kobayashi, K., Satrústegui, J., and Saheki, T. (2005) Reduced N-acetylaspartate levels in mice lacking aralar, a brain- and muscle-type mitochondrial aspartate-glutamate carrier. *J. Biol. Chem.* **280**, 31333–31339
- Rogers, G. W., Brand, M. D., Petrosyan, S., Ashok, D., Elorza, A. A., Ferrick, D. A., and Murphy, A. N. (2011) High throughput microplate respiratory measurements using minimal quantities of isolated mitochondria. *PLoS One* **6**, e21746
- Asimakis, G. K., and Aprille, J. R. (1980) *In vitro* alteration of the size of the liver mitochondrial adenine nucleotide pool. Correlation with respiratory functions. *Arch. Biochem. Biophys.* **203**, 307–316
- D'Souza, M. P., and Wilson, D. F. (1982) Adenine nucleotide efflux in mitochondria induced by inorganic pyrophosphate. *Biochim. Biophys. Acta* **680**, 28–32
- Gómez-Galán, M., Makarova, J., Llorente-Folch, I., Saheki, T., Pardo, B., Satrústegui, J., and Herreras, O. (2012) Altered postnatal development of cortico-hippocampal neuronal electric activity in mice deficient for the mitochondrial aspartate-glutamate transporter. *J. Cereb. Blood Flow Metab.* **32**, 306–317
- Traba, J., Del Arco, A., Duchon, M. R., Szabadkai, G., and Satrústegui, J. (2012) SCaMC-1 promotes cancer cell survival by desensitizing mitochondrial permeability transition via ATP/ADP-mediated matrix  $\text{Ca}^{2+}$  buffering. *Cell Death Differ.* **19**, 650–660
- Mármol, P., Pardo, B., Wiederkehr, A., del Arco, A., Wollheim, C. B., and Satrústegui, J. (2009) Requirement for aralar and its  $\text{Ca}^{2+}$ -binding sites in  $\text{Ca}^{2+}$  signal transduction in mitochondria from INS-1 clonal  $\beta$ -cells. *J. Biol. Chem.* **284**, 515–524
- Anunciado-Koza, R. P., Zhang, J., Ukropec, J., Bajpeyi, S., Koza, R. A., Rogers, R. C., Cefalu, W. T., Mynatt, R. L., and Kozak, L. P. (2011) Inactivation of the mitochondrial carrier slc25a25 (ATP-Mg $^{2+}$ / $\text{P}_i$  transporter) reduces physical endurance and metabolic efficiency in mice. *J. Biol. Chem.* **286**, 11659–11671
- Kokoszka, J. E., Waymire, K. G., Levy, S. E., Sligh, J. E., Cai, J., Jones, D. P.,

## SCaMC-3 Is a Mitochondrial Target of Glucagon

- MacGregor, G. R., and Wallace, D. C. (2004) The ADP/ATP translocator is not essential for the mitochondrial permeability transition pore. *Nature* **427**, 461–465
32. Hunter D. R., and Haworth R. A. (1979) The  $\text{Ca}^{2+}$ -induced membrane transition in mitochondria. I. The protective mechanisms. *Arch Biochem. Biophys* **195**, 453–459
33. Gizatullina, Z. Z., Chen, Y., Zierz, S., and Gellerich, F. N. (2005) Effects of extramitochondrial ADP on permeability transition of mouse liver mitochondria. *Biochim. Biophys. Acta* **1706**, 98–104
34. Chinopoulos, C., and Adam-Vizi, V. (2010) Mitochondrial  $\text{Ca}^{2+}$  sequestration and precipitation revisited. *FEBS J* **277**, 3637–3651
35. Valcarce, C., and Cuezva, J. M. (1991) Interaction of adenine nucleotides with the adenine nucleotide translocase regulates the developmental changes in proton conductance of the inner mitochondrial membrane. *FEBS Lett.* **294**, 225–228
36. Nosek, M. T., and Aprille, J. R. (1992) ATP-Mg/ $\text{P}_i$  carrier activity in rat liver mitochondria. *Arch. Biochem. Biophys.* **296**, 691–697
37. Dransfield, D. T., and Aprille, J. R. (1993) Regulation of the mitochondrial ATP-Mg/ $\text{P}_i$  carrier in isolated hepatocytes. *Am. J. Physiol.* **264**, C663–670
38. Morgan, N. G., Charest, R., Blackmore, P. F., and Exton, J. H. (1984) Potentiation of  $\alpha 1$ -adrenergic responses in rat liver by a camp-dependent mechanism. *Proc. Natl. Acad. Sci. U.S.A.* **81**, 4208–4212
39. Hamman, H. C., and Haynes, R. C., Jr. (1983) Elevated intramitochondrial adenine nucleotides and mitochondrial function. *Arch. Biochem. Biophys.* **223**, 85–94
40. Soboll, S., and Scholz, R. (1986) Control of energy metabolism by glucagon and adrenaline in perfused rat liver. *FEBS Lett.* **205**, 109–112
41. Prpić, V., Spencer, T. L., and Bygrave, F. L. (1978) Stable enhancement of Calcium retention in mitochondria isolated from rat liver after the administration of glucagon to the intact animal. *Biochem. J.* **176**, 705–714
42. Assimacopoulos-Jeannet, F., McCormack, J. G., and Jeanrenaud, B. (1986) Vasopressin and/or glucagon rapidly increases mitochondrial calcium and oxidative enzyme activities in the perfused rat liver. *J. Biol. Chem.* **261**, 8799–8804
43. McCormack, J. G., Halestrap, A. P., and Denton, R. M. (1990) Role of calcium ions in regulation of mammalian intramitochondrial metabolism. *Physiol. Rev.* **70**, 391–425
44. Yamazaki, R. K. (1975) Glucagon stimulation of mitochondrial respiration. *J. Biol. Chem.* **250**, 7924–7930
45. Halestrap, A. P. (1987) Glucagon treatment of rats activates the respiratory chain of liver mitochondria at more than one site. *Biochim. Biophys. Acta* **927**, 280–290
46. Sutton, R., and Pollak, J. K. (1978) The increasing adenine nucleotide concentration and the maturation of rat liver mitochondria during neonatal development. *Differentiation* **12**, 15–21
47. Carafoli, E., Rossi, C. S., and Lehninger, A. L. (1965) Uptake of adenine nucleotides by respiring mitochondria during active accumulation of  $\text{Ca}^{2+}$  and phosphate. *J. Biol. Chem.* **240**, 2254–2261
48. Halestrap, A. P. (1982) The nature of the stimulation of the respiratory chain of rat liver mitochondria by glucagon pretreatment of animals. *Biochem. J.* **204**, 37–47
49. Halestrap, A. P. (1989) The regulation of the matrix volume of mammalian mitochondria *in vivo* and *in vitro* and its role in the control of mitochondrial metabolism. *Biochim. Biophys. Acta* **973**, 355–382
50. Garlid, K. D., and Halestrap, A. P. (2012) The mitochondrial  $\text{K}^+$ (ATP) channel. Fact or fiction? *J. Mol. Cell. Cardiol.* **52**, 578–583
51. Balaban, R. S. (2012) Perspectives on SGP symposium on mitochondrial physiology and medicine. Metabolic homeostasis of the heart. *J. Gen. Physiol.* **139**, 407–414
52. Crompton, M., and Goldstone, T. P. (1986) The involvement of calcium in the stimulation of respiration in isolated rat hepatocytes by adrenergic agonists and glucagon. *FEBS Lett.* **204**, 198–202
53. Quinlan, P. T., Thomas, A. P., Armston, A. E., and Halestrap, A. P. (1983) Measurement of the intramitochondrial volume in hepatocytes without cell disruption and its elevation by hormones and valinomycin. *Biochem. J.* **214**, 395–404